JACS
JOURNAL OF THE AMERICAN CHEMICAL SOCIETY
Communication
pubs.acs.org/JACS

Anchoring a Molecular Iron Catalyst to Solar-Responsive WO_3 Improves the Rate and Selectivity of Photoelectrochemical Water Oxidation

Benjamin M. Klepser and Bart M. Bartlett*

Department of Chemistry, University of Michigan, 930 North University Avenue, Ann Arbor, Michigan 48109, United States

Supporting Information

ABSTRACT: Molecular catalysts help overcome the kinetic limitations of water oxidation and generally result in faster rates for water oxidation than do heterogeneous catalysts. However, molecular catalysts typically function in the dark and therefore require sacrificial oxidants such as Ce^{4+} or $S_2O_8^{2-}$ to provide the driving force for the reaction. In this Communication, covalently anchoring a phosphonate-derivatized complex, Fe(tebppmcn)Cl_2 (**1**), to WO_3 removes the need for a sacrificial oxidant and increases the rate of photoelectrochemical water oxidation on WO_3 by 60%. The dual-action catalyst, **1**-WO_3, also gives rise to increased selectivity for water oxidation in pH 3 Na_2SO_4 (56% on bare WO_3, 79% on **1**-WO_3). This approach provides promising alternative routes for solar water oxidation.

Overall, water photolysis has been proposed as a potentially viable route to generating hydrogen fuel. However, catalyzing the water oxidation half-reaction remains a major obstacle. Both molecular and heterogeneous catalysts have been developed for catalyzing water oxidation, but both suffer from drawbacks.[1,2] Molecular water oxidation catalysts (WOCs) were first reported by Meyer and co-workers with the discovery of the ruthenium "blue dimer",[3] and they have garnered renewed interest with the development of metal complexes capable of oxidizing water as fast as enzymes.[4,5] The first report of a non-noble metal molecular WOC was a manganese dimer developed by Crabtree, Brudvig, and co-workers.[6] Since this report, there are several examples of iron,[7,8] cobalt,[9−11] and copper[5,12] WOCs. Molecular catalysts are attractive because they are easily modified[13] and reaction kinetics are measured straightforwardly.[14] However, many molecular water oxidation catalysts are not photocatalysts without adding a photosensitizer. Consequently, most rely on using sacrificial oxidants.[3−14] The only examples of molecular complexes oxidizing water without sacrificial oxidants require electrochemical oxidation of those catalysts.[5,12] In contrast, heterogeneous photocatalysts such as TiO_2, WO_3, Fe_2O_3, etc. are inherently photoactive and can perform overall water splitting (with an additional bias if necessary).[15] The distinct advantage of metal oxide semiconductors is that they generally exhibit excellent chemical stability in aqueous solution. However, semiconductor photocatalysts are not always kinetically selective for water oxidation,[16,17] and elucidation of the reaction mechanisms is much more challenging.[18]

To overcome these challenges, we report the synthesis of a modified molecular iron catalyst, Fe(tebppmcn)Cl_2 (tebppmcn = tetraethyl *N,N′*-bis(2-methylpyridyl-4-phosphonate)-*N,N′*-dimethylcyclohexyldiamine), (**1**) with a phosphonate linkage to attach the molecule to WO_3 photoelectrodes for water oxidation. The $[Fe(bpmcn)]^{2+}$ (bpmcn = *N,N′*-bis(2-methylpyridyl)-*N,N′*-dimethylcyclohexyldiamine) complex without the tether (**2**) was first reported by Chen and Que[19] as a hydrocarbon oxidation catalyst,[20] and has also been reported as a dark water oxidation catalyst by Fillol et al.[8] New to this manuscript, we find that covalently anchoring the molecular iron complex to the surface of WO_3 electrodes increases both the photocurrent density (j_{ph}) generated in semiconducting WO_3 and the Faradaic efficiency ($\eta(O_2)$) for water oxidation. This result suggests that light-absorbing semiconductors can be used to photo-oxidize the molecular complex, and this strategy could be implemented to photocatalyze other oxidation reactions with molecular catalysts in place of sacrificial chemical oxidants.

Recently, a molecular ruthenium catalyst tethered to Fe_2O_3 was communicated.[21] However, in this report, no evidence for oxygen evolution is presented. Furthermore, this report did not demonstrate prolonged stability of the anchors under illumination or under an applied bias in aqueous solutions. Carboxylate anchors were used to attach the Ru complex to the Fe_2O_3 surface, and carboxylate anchors typically suffer from weak surface attachment in aqueous solutions.[22] Our work focuses on phosphonate anchors that demonstrate improved stability,[23] and oxygen evolution has been monitored and correlated to greater Faradaic efficiency for the modified electrodes over 3 h of photoelectrolysis using simulated solar illumination.

With regard to synthesis, there are very few examples of modifying the *para* position on the pyridine rings for the *N,N′*-bis(2-methylpyridyl)-*N,N′*-dimethylethylenediamine class of ligands.[24] However, adapting the traditional syntheses used to generate this class of ligands was successful for preparing the desired phosphonate-modified complexes. After quantitative transformation of the *ortho* $-CH_2OH$ substituent on the pyridine ring to $-CH_2Cl$, 2 equiv of this *o*-chloromethylpyridine reacted moderately (up to 62%) with the deprotonated secondary diamine to afford the desired modified ligand in two steps from the hydroxymethylpyridine as depicted in Scheme 1. Metalation proceeded in high yields, and was fast as characterized

Received: August 21, 2013
Published: January 17, 2014

dx.doi.org/10.1021/ja4086808 | *J. Am. Chem. Soc.* 2014, 136, 1694−1697

Scheme 1. Synthesis of Fe(R-bpmcn)Cl_2

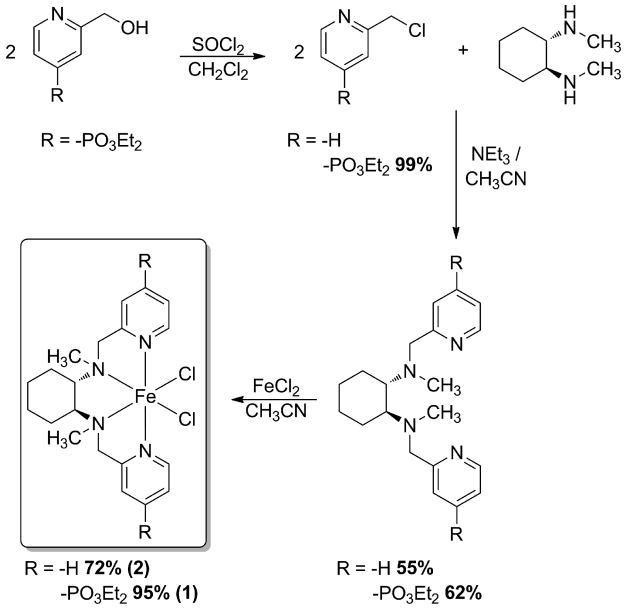

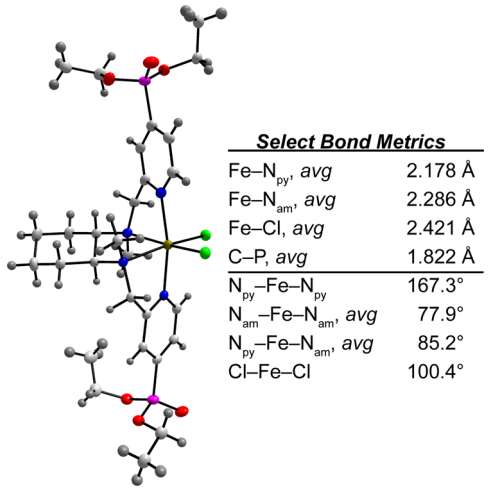

Figure 1. X-ray crystal structure of **1** where C = white, H = gray, N = blue, O = red, P = magenta, Cl = green, Fe = yellow.

by a rapid color change from orange to purple or yellow for complexes **1** and **2**, respectively.

X-ray crystallography shows the desired structure of complex **1**, in Figure 1, and elemental analysis confirms the purity. The solution electrochemical behaviors of **1** and **2** (Figure S1) are similar to what has been reported for similar complexes.[25] Furthermore, complexes **1** and **2** exhibit similar reactivity toward water oxidation in the presence of the sacrificial oxidant, $(NH_4)_2Ce(NO_3)_6$, as reported by Fillol et al.,[8] illustrated in Figure 2. For example, after 30 min of stirring in the dark, complexes **1** and **2** show 85 and 113 turnovers, respectively. Despite having slightly lower stability relative to complex **2**, the initial rate of water oxidation is comparable for complexes **1** and **2**.

The phosphonate-modified complex, **1**, was anchored to WO_3 by soaking the electrodes in 0.50 mM **1**/acetonitrile at 80 °C for 8 h. WO_3 electrodes were prepared by a sol–gel synthesis as previously reported.[26] Although the UV–vis diffuse reflectance of the films is largely unchanged due to the thin nature of the

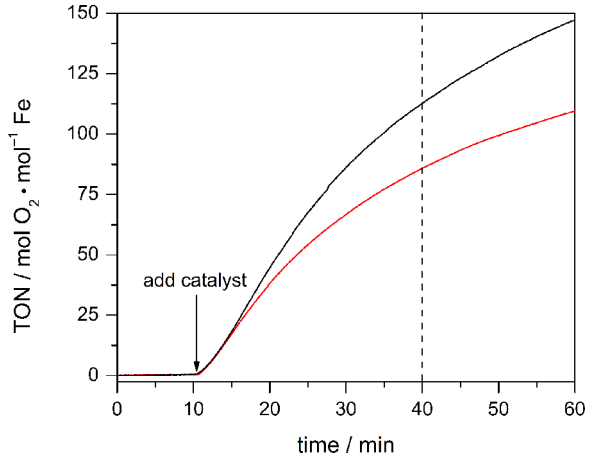

Figure 2. Homogeneous water oxidation of 12.5 μM complex **2** (black) and **1** (red) in 12.5 mM $(NH_4)_2Ce(NO_3)_6$ aqueous solutions.

films, the Raman spectrum (Figure S2) shows that complex **1** is bound to the WO_3 electrode. In addition, the cyclic voltammetry of the freshly modified electrodes (Figure S3) exhibits a set of redox waves at −0.18 V vs $Fc^{+/0}$, which is consistent with solution electrochemistry, but is covered by a redox event from WO_3 at −0.3 V vs $Fc^{+/0}$. There is also evidence of a slight anodic peak at 0.75 V vs $Fc^{+/0}$, which is consistent with irreversible $Fe^{3+/4+}$ oxidation in acetonitrile electrolytes containing **1**. These assignments have been verified by low temperature EPR spectroscopy in nonaqueous electrolytes (Figure S4). Coulometry carried out at 0.43 V vs $Fc^{+/0}$ reveals the surface coverage of the complex is ∼15 nmol/cm^2 (Figure S5). Because catalyst **1** should be an electrocatalyst, the dark linear sweep voltammetry of **1**-WO_3 was compared to that of bare WO_3, and no noticeable difference was observed between the two electrodes (Figure S6). This result is most likely due to low surface coverage of **1** such that the catalyst is unable to out-perform the high surface area semiconductor. Also noteworthy is that **1** tethered directly to the underlying FTO conducting substrate behaves as an electrocatalyst only at high bias (>1.6 V vs RHE).

Confident that the WO_3 electrode is modified with **1**, the photoelectrochemical performance of modified electrodes (**1**-WO_3) is directly compared to the same films prior to modification in pH 3 Na_2SO_4. The **1**-WO_3 electrodes exhibit a significant, reproducible increase in photocurrent of ∼60%. The linear sweep voltammetry for a single representative film before and after anchoring the complex is illustrated in Figure 3. Furthermore, we have carried out three control experiments: if a WO_3 electrode is soaked in acetonitrile in the absence of **1**, with only $FeCl_2$, or with only the tebppmcn ligand without iron present, and then dried, there is no increase in the photocurrent density on WO_3 (Figure S7). *Therefore, anchoring complex 1 is necessary to observe an increase in photocurrent density on the electrode.* The saturated photocurrent is consistent with excellent charge-carrier separation in WO_3, and the increase in photocurrent is indicative of a faster chemical reaction in the presence of the molecular catalyst. These findings also demonstrate that the photogenerated holes from WO_3 are rapidly oxidizing the molecular complex on the surface in place of a sacrificial oxidant.

To rule out the possibility that WO_3 performance alone results in faster reaction rate, we varied the thickness of the film to control the photocurrent density.[26] The optimized thickness of WO_3 was ∼1.8 μm by SEM imaging (Figure S8), and the thinner film was ∼0.6 μm. Although thinner films gives rise to lower

dx.doi.org/10.1021/ja4086808 | J. Am. Chem. Soc. 2014, 136, 1694–1697

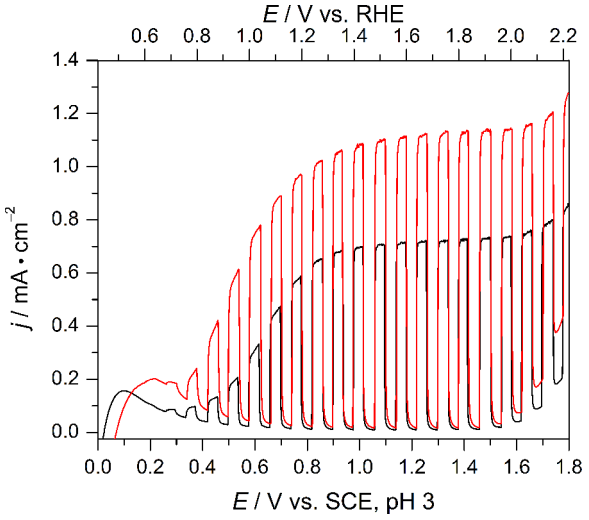

Figure 3. Chopped light linear sweep voltammetry of a WO_3 film as prepared (black) and after modification with **1** (red) in pH 3 0.1 M Na_2SO_4, 100 mW cm^{-2} AM 1.5G illumination, 20 mV/s, Pt CE, SCE RE.

photocurrent density, as expected, thinner films of WO_3 still demonstrated a 50% increase in photocurrent density when modified with **1** (Figure S9). This suggests that the role of the semiconductor is primarily to photooxidize the molecule to form the catalytically active species. Moreover, this results shows that the rate is limited by the rate of catalyst formation.

Furthermore, it has been demonstrated previously that complex **2** loses reactivity under more basic (pH >7) photocatalytic reaction conditions.[27] Therefore, the stability of **1**-WO_3 was examined under various pH. Upon adjusting the pH of the electrolyte from 1 to 7, we observed that the jump in photocurrent decreases slightly as pH increases from 1 to 5 (Figure S10). However, increasing the pH to 7 results in a large decrease in photocurrent enhancement (from ∼50% to ∼20%). This decreased performance suggests that either the complex is becoming less active or is desorbing from the WO_3 surface. Alternatively, this decrease at pH 7 could be attributed to the relative instability of WO_3 above pH 6. To distinguish among these possibilities, we are now synthesizing different anchors that are known to be stable on oxide semiconductor surfaces and different semiconductors that are stable over a wider pH range.

One problem typically encountered with WO_3 is that water oxidation is slow under acidic conditions causing electrolyte oxidation to become a competitive side reaction, as has been previously studied.[16] Accordingly, the Faradaic efficiency for O_2 evolution is significantly reduced. However, a molecular catalyst is generally more selective toward a specific reaction than heterogeneous oxide-based catalysts, and **1** oxidizes water in the presence of Ce^{4+} (1.72 V vs RHE). As such, we predicted that the Faradaic efficiency for O_2 evolution on **1**-WO_3 electrodes should be higher than that of the bare WO_3 electrode.

Oxygen detection, measured with a fluorescence lifetime probe, indeed shows a significant increase in Faradaic efficiency of **1**-WO_3 electrodes relative to the control WO_3 electrodes ($\eta(O_2)$ = 79 ± 9% for **1**-WO_3 and $\eta(O_2)$ = 56 ± 7% for WO_3, summarized in Table S1), and representative examples are depicted in Figure 4. With a catalyst present, there is a large increase in the selectivity of the modified electrode toward water oxidation. To demonstrate the repeatability of film production and performance, O_2 evolution data for two different **1**-WO_3

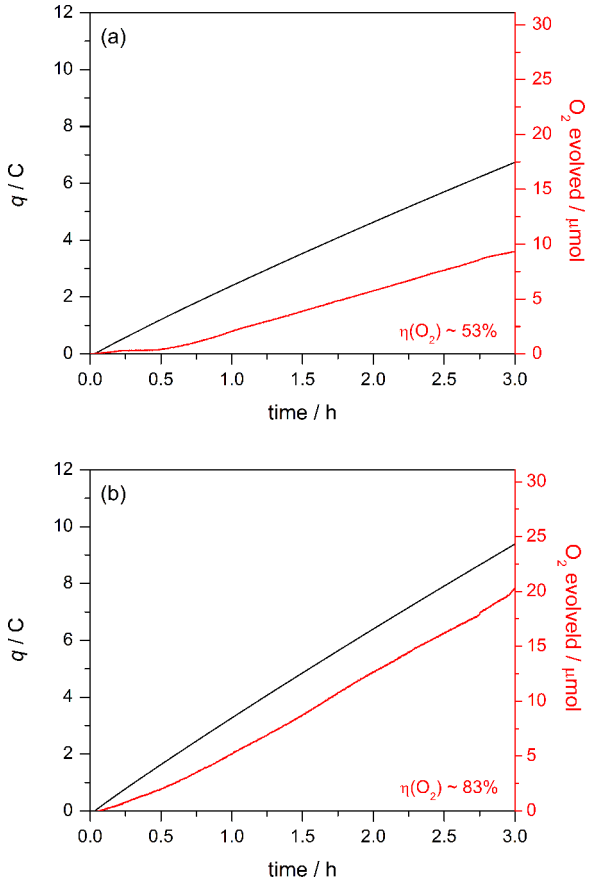

Figure 4. Faradaic efficiency of bare (a) and **1**-modified (b) WO_3 electrodes in pH 3 Na_2SO_4 under 100 mW cm^{-2} AM 1.5G electrolysis at 1.23 V vs NHE, Pt CE, SCE RE; the theoretical maximum O_2 based on charge passed (black) and the amount of O_2 produced (red).

films are presented in Figure S11. Furthermore, **1**-WO_3 maintains high Faradaic efficiency for up to 12 h under illumination (Figure S12). The Faradaic efficiency was not improved after modifying WO_3 with only the tebppmcn ligand (Figure S13), implying that iron is required.

To verify the increased efficiency of the modified **1**-WO_3 electrodes further, the quantity of other non-O_2 oxidized species (e.g., $S_2O_8^{2-}$, H_2O_2, or HSO_5^-) was determined spectroscopically by adding $Fe(SCN)_2$ and excess NaSCN, then measuring the concentration of the deep red oxidized species in solution.[16] The efficiency for generating other species is η(non-O_2) = 22% and η(non-O_2) = 37% for **1**-WO_3 and WO_3 electrodes respectively. These long-term experiments demonstrate the higher reactivity of the catalyst toward water oxidation on the electrode surface under illumination. Additionally, the catalyst **1**-WO_3 is performing the photooxidation of water in the absence of other sacrificial oxidants.

In solution, the previously reported, unmodified complex **2** decomposes by ligand hydrolysis or oxidation,[8] and we note that after photoelectrolysis for 3 h, the Raman and UV−vis spectra (Figure S2), cyclic voltammetry (Figure S3), and XP spectoscopy (Figure S14) show no features consistent with the presence of **1** on the WO_3 surface. These observations do not preclude the presence of a trace amount of catalyst remaining bound to the surface, but we also acknowledge that complex **1** tethered to WO_3 may be a mere precatalyst for water oxidation. Regardless, the rate enhancement and selectivity are noteworthy. In order to provide evidence that a catalytically active species

dx.doi.org/10.1021/ja4086808 | J. Am. Chem. Soc. 2014, 136, 1694−1697

remains *on the WO_3 surface* after oxygen evolution, the Faradaic efficiency of a **1**-WO_3 electrode was measured for 3 h, then the electrolyte was discarded, fresh degassed electrolyte was introduced into the cell, and oxygen evolution from the same **1**-WO_3 film was repeated for another 3 h. After this second photoelectrolysis, the increase in Faradaic efficiency for oxygen evolution remains (Figure S15). Moreover, when the Faradaic efficiency of an unmodified WO_3 electrode was measured in the presence of freely diffusing 0.5 μM **1** (10 nmol in 20 mL) there is no improvement of the Faradaic efficiency for water oxidation (Figure S16). Although we cannot say unequivocally that **1** is the true catalyst these results support the assertion that the active species remains on the WO_3 surface and is not freely diffusing in the electrolyte.

One final point of note is that at pH 3, any iron species removed from the electrode surface is soluble in water. ESI mass spectrometry of the electrolyte following photoelectrolysis only shows peaks corresponding to **1**, including the hydrolysis of the phosphonate esters, as mostly Fe^{V} or Fe^{VI} fragments (Figure S17). A CV of the supporting electrolyte further supports high valent iron dissociating during photoelectrolysis (Figure S18). Although some of the complex dissociates from the surface, SEM imaging also shows no obvious evidence of new nanoparticles growing on the WO_3 surface or change in the morphology of WO_3 after oxygen evolution (Figure S19). These data support the notion that the catalyst is not decomposing to form Fe_2O_3 under illumination in the presence of oxidative holes from WO_3.

In conclusion, we have demonstrated successfully combining an earth-abundant molecular catalyst, Fe(tebppmcn)Cl_2 (**1**), with the semiconducting photoelectrode, WO_3, dramatically increases the rate and selectivity of photoelectrochemical water oxidation. Furthermore, we remove the need for a sacrificial chemical oxidant such as Ce^{4+}. These results reveal the promise of enhancing water oxidation using catalytically active molecular complexes anchored onto stable, solar-responsive semiconductors.

■ ASSOCIATED CONTENT

Ⓢ Supporting Information

Experimental procedures, UV−vis and Raman spectra, cyclic voltammograms, O_2 evolution data, SEM images, and a CIF file. This material is available free of charge via the Internet at http://pubs.acs.org.

■ AUTHOR INFORMATION

Corresponding Author

bartmb@umich.edu

Notes

The authors declare no competing financial interest.

■ ACKNOWLEDGMENTS

This research was supported by a grant from the United States Department of Energy (DE-FG02-11ER16262). We thank Dr. Jeff W. Kampf for assistance with X-ray crystallography.

■ REFERENCES

(1) Reviews of molecular WOCs: (a) Brimblecombe, R.; Dismukes, G. C.; Swiegers, G. F.; Spiccia, L. *Dalton Trans.* **2009**, 9374. (b) Duan, L.; Tong, L.; Xu, Y.; Sun, L. *Energy Environ. Sci.* **2011**, *4*, 3296.

(2) Reviews of heterogeneous WOCs: (a) Walter, M. G.; Warren, E. L.; McKone, J. R.; Boettcher, S. W.; Mi, Q.; Santori, E. A.; Lewis, N. S. *Chem. Rev.* **2010**, *110*, 6446. (b) Kudo, A.; Miseki, Y. *Chem. Soc. Rev.* **2009**, *38*, 253.

(3) Gersten, S. W.; Samuels, G. J.; Meyer, T. J. *J. Am. Chem. Soc.* **1982**, *104*, 4029.

(4) Duan, L.; Bozoglian, F.; Mandal, S.; Stewart, B.; Privalov, T.; Llobet, A.; Sun, L. *Nat. Chem.* **2012**, *4*, 418.

(5) Barnett, S. M.; Goldberg, K. I.; Mayer, J. M. *Nat. Chem.* **2012**, *4*, 498.

(6) Limburg, J.; Vrettos, J. S.; Liable-Sands, L. M.; Rheingold, A. L.; Crabtree, R. H.; Brudvig, G. W. *Science* **1999**, *283*, 1524.

(7) Ellis, W. C.; McDaniel, N. D.; Bernhard, S.; Collins, T. J. *J. Am. Chem. Soc.* **2010**, *132*, 10990.

(8) Fillol, J. L.; Codolá, Z.; Garcia-Bosch, I.; Gómez, L.; Pla, J. J.; Costas, M. *Nat. Chem.* **2011**, *3*, 807.

(9) McCool, N. S.; Robinson, D. M.; Sheats, J. E.; Dismukes, G. C. *J. Am. Chem. Soc.* **2011**, *133*, 11446.

(10) Wasylenko, D. J.; Palmer, R. D.; Schott, E.; Berlinguette, C. P. *Chem. Commun.* **2011**, *47*, 4249.

(11) Hong, D.; Jung, J.; Park, J.; Yamada, Y.; Suenobu, T.; Lee, Y.; Nam, W.; Fukuzumi, S. *Energy Environ. Sci.* **2012**, *5*, 7607.

(12) Zhang, M.-T.; Chen, Z.; Kang, P.; Meyer, T. J. *J. Am. Chem. Soc.* **2013**, *135*, 2048.

(13) Zong, R.; Thummel, R. P. *J. Am. Chem. Soc.* **2005**, *127*, 12802−12803.

(14) Representative examples: (a) Wasylenko, D. J.; Ganesamoorthy, C.; Koivisto, B. D.; Henderson, M. A.; Berlinguette, C. P. *Inorg. Chem.* **2010**, *49*, 2202. (b) Concepcion, J. J.; Jurss, J. W.; Templeton, J. L.; Meyer, T. J. *J. Am. Chem. Soc.* **2008**, *130*, 16462. (c) Duan, L.; Xu, Y.; Tong, L.; Sun, L. *Chem. Sus. Chem.* **2011**, *4*, 238.

(15) (a) Fujishima, A.; Honda, K. *Nature* **1972**, *238*, 37. (b) Butler, M. A.; Nasby, R. D.; Quinn, R. K. *Solid State Commun.* **1976**, *19*, 1011. (c) Hardee, K. L.; Bard, A. J. *J. Electrochem. Soc.* **1976**, *123*, 1024.

(16) Mi, Q.; Zhanaidarova, A.; Brunschwig, B. S.; Gray, H. B.; Lewis, N. S. *Energy Environ. Sci.* **2012**, *5*, 5694.

(17) (a) Hill, J. C.; Choi, K.-S. *J. Phys. Chem. C* **2012**, *116*, 7612. (b) Mi, Q.; Coridan, R. H.; Bruschwig, B. S.; Gray, H. B.; Lewis, N. S. *Energy Environ. Sci.* **2013**, *6*, 2646.

(18) Klahr, B.; Gimenez, S.; Fabregat-Santiago, F.; Bisquert, J.; Hamann, T. W. *Energy Environ. Sci.* **2012**, *5*, 7626.

(19) Chen, K.; Que, L., Jr. *Chem. Commun.* **1999**, 1375.

(20) (a) Costas, M.; Tipton, A. K.; Chen, K.; Jo, D.-H.; Que, L., Jr. *J. Am. Chem. Soc.* **2001**, *123*, 6722. (b) Costas, M.; Que, L., Jr. *Angew. Chem., Int. Ed.* **2002**, *41*, 2179.

(21) Chen, X.; Ren, X.; Liu, Z.; Zhuang, L.; Lu, J. *Electrochem. Commun.* **2013**, *27*, 148.

(22) Representative examples: (a) Gillaizeau-Gauthier, I.; Odobel, F.; Alebbi, M.; Argazzi, R.; Costa, E.; Bignozzi, C. A.; Qu, P.; Meyer, G. J. *Inorg. Chem.* **2001**, *40*, 6073. (b) Park, H.; Bae, E.; Lee, J.-J.; Park, J.; Choi, W. *J. Phys. Chem. B* **2006**, *110*, 8740.

(23) Representative examples: (a) Chen, Z.; Concepcion, J. J.; Jurss, J. W.; Meyer, T. J. *J. Am. Chem. Soc.* **2009**, *131*, 15580. (b) Lee, S-H. A.; Zhao, Y.; Hernandez-Pagan, E. A.; Blasdel, L.; Youngblood, W. J.; Mallouk, T. E. *Faraday Discuss.* **2012**, *155*, 165. (c) Giokas, P. G.; Miller, S. A.; Hanson, K.; Norris, M. R.; Glasson, C. R. K.; Concepcion, J. J.; Bettis, S. E.; Meyer, T. J.; Moran, A. M. *J. Phys. Chem. C* **2013**, *117*, 812.

(24) (a) Delroisse, M.; Rabion, A.; Chardac, F.; Tétard, D.; Verlhac, J.-B.; Fraisse, L.; Séris, J.-L. *J. Chem. Soc., Chem. Commun.* **1995**, 949. (b) Mialane, P.; Tchertanov, L.; Banse, F.; Sainton, J.; Girerd, J.-J. *Inorg. Chem.* **2000**, *39*, 2440. (c) England, J.; Gondhia, R.; Bigorra-Lopez, L.; Petersen, A. R.; White, A. J. P.; Britovsek, G. J. P. *Dalton Trans.* **2009**, 5319.

(25) Coates, C. M.; Hagan, K.; Mitchell, C. A.; Gorden, J. D.; Goldsmith, C. R. *Dalton Trans.* **2011**, *40*, 4048.

(26) Santato, C.; Odziemkowski, M.; Ulmann, M.; Augustynski, J. *J. Am. Chem. Soc.* **2001**, *123*, 10639.

(27) Chen, G.; Chen, J.; Ng, S.-M.; Man, W.-L.; Lau, T.-C. *Angew. Chem., Int. Ed.* **2013**, *52*, 1.